Effect of neutron–photon converter materials (Cd, Gd, and Sm) on the positron production in a reactor-based slow positron beamline

Atsushi Yabuuchi*

Institute for Integrated Radiation and Nuclear Science, Kyoto University, Kumatori, Osaka 590–0494, Japan

Abstract

The change in the amount of positron production when Cd cap, installed as a neutron–photon converter, is replaced with Gd or Sm caps was simulated by Monte Carlo calculations in the slow positron beamline at the Kyoto University Research Reactor, especially focusing on the change in the amount of positron production induced by neutrons emitted from a reactor core. Based on the simulation results, the amount of positron production induced by neutrons obtained using Gd and Sm caps was estimated to decrease to (69 ± 4)% and (54 ± 3)%, respectively, compared with the amount obtained using Cd cap. Meanwhile, Cd and Gd caps with a thickness of 1 mm were evaluated to have almost the same burn-up lifetime. Therefore, a Cd cap is the best choice, while a Gd cap, which has a higher melting point, could be an alternative if the structure of the positron source makes effective cooling difficult.

Keywords: Reactor-based slow positron beamline, Neutron capture gamma-ray, Pair production, Monte Carlo simulation

1. Introduction

Positrons are useful to detect vacancy-type defects in thin films and near the surface of materials with high sensitivity [1, 2, 3, 4]. An intense slow positron beam enables the use of positrons in advanced measurement techniques beyond conventional positron annihilation measurements, such as scanning positron microscopy [5, 6, 7, 8, 9] and total reflection high-energy positron diffraction [10, 11, 12]. Therefore, the operation and/or the new construction of intense slow positron beam facilities using nuclear reactors as a positron source are being promoted in many countries [13, 14, 15, 16, 17, 18, 19, 20, 21, 22, 23, 24]. Experimental and simulation studies on positron moderation for a reactor-based positron source were also conducted [16, 25]. In reactor-based slow positron beamlines, a neutron–photon converter made of cadmium (Cd) is commonly used to improve the intensity of gamma-ray photons required for the positron pair production [13, 14, 15, 16, 17, 18, 19, 20, 21]. A reactor-based positron source containing a neutron–photon converter is exposed to an intense nuclear heating environment. As Cd has a relatively low melting point (321°C), the positron source must be designed with sufficient consideration for its cooling [26].

Besides Cd, gadolinium (Gd) and samarium (Sm) are candidate materials with a large thermal neutron capture cross-section and prompt gamma-ray photon emission [27]. Table 1 summarizes the thermal neutron radiative capture cross-sections and natural abundance ratios for each nuclide [28]. The gamma-ray intensity at a reactor-based positron source is improved through the ^{113}Cd(n,γ)^{114}Cd reaction, but it will also be improved through ^{157}Gd(n,γ)^{158}Gd, ^{155}Gd(n,γ)^{156}Gd, and ^{149}Sm(n,γ)^{150}Sm reactions. Gd and Sm have melting points of 1312°C and 1072°C, respectively; thus, unlike Cd, there is no need to be concerned about melting. In this study, taking the slow positron beamline at the Kyoto University Research Reactor (KUR) as an example, changes in the amount of positron pair production when using Gd or Sm instead of Cd as the neutron–photon conversion material were calculated using Monte Carlo simulations, especially focusing on the change in the amount of positron production induced by neutrons emitted from a reactor core. In addition, the burn-up lifetimes of Cd, Gd, and Sm converters used as neutron–photon conversion materials at the KUR positron source were evaluated. Evaluation results found that using Cd is the best choice when the amount of positron pair production is the primary consideration; however, Gd can be a useful alternative in some situations.

Table 1: Thermal neutron radiative capture cross-sections and natural abundances for each nuclide.

Nuclide	Cross-section (b)	Natural abundance (%)
^{113}Cd	20,600	12.22
^{157}Gd	254,000	15.65
^{155}Gd	60,900	14.80
^{149}Sm	40,140	13.82

2. Simulation method

Fig. 1 shows a schematic view of the KUR slow positron beamline. The KUR is a light water-moderated tank-type re-

*Corresponding author
Email address: yabuuchi@rri.kyoto-u.ac.jp (Atsushi Yabuuchi)

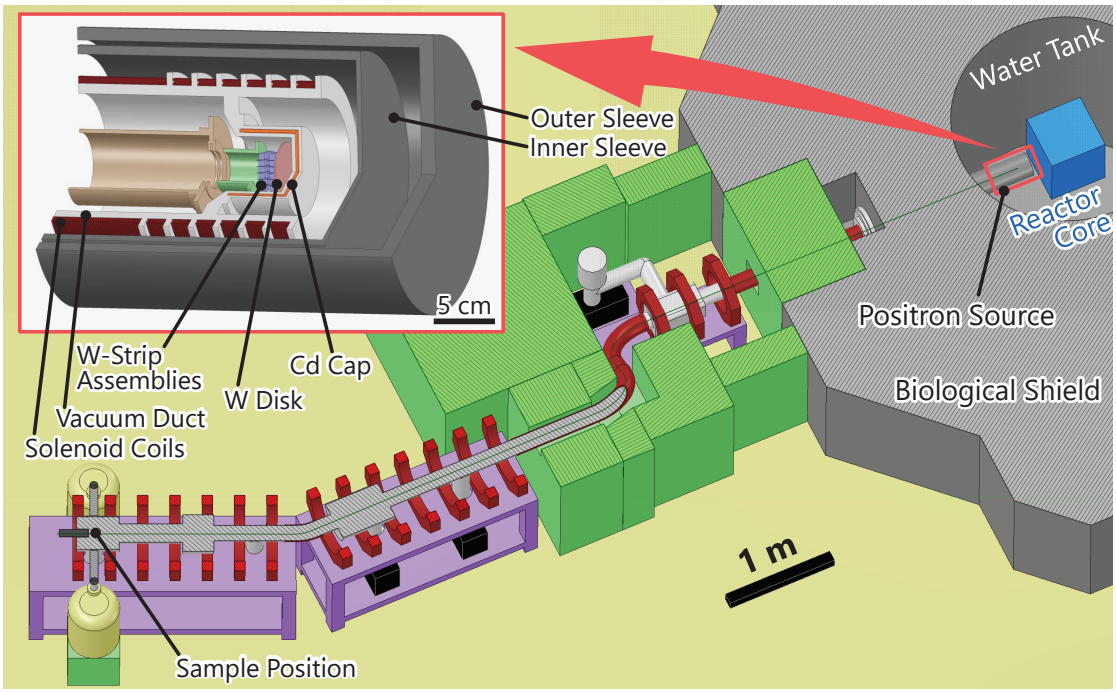

Figure 1: Schematic view of the KUR slow positron beamline. Positrons are produced at the end of a vacuum duct that extends close to the reactor core. Positrons moderated at the positron source are guided by a magnetic field and transported to the sample position as a slow positron beam. The rectangular frame at the upper left of the panel shows a magnified view of the positron source at the end of the vacuum duct. W disk and W-strip assemblies are installed as a photon–positron converter and positron moderator, respectively. A Cd cap surrounds the W disk to use neutron capture-induced prompt gamma-ray photons as well as fission gamma-ray photons for positron pair production. The inner sleeve is inserted to protect the outer sleeve, which is part of the reactor, from severe earthquakes.

actor; the reactor core consisting of fuel elements is cooled by light water. The KUR has a maximum thermal power of 5 MW and is available in 1-MW or 5-MW operation modes, but, most of the time, it is operated at 1 MW. At the experimental hole for a slow positron beam, the vacuum duct extends close to the reactor core. The space between the vacuum duct and the inner sleeve is filled with air or He gas [26], whereas the space between the inner and outer sleeves is filled with air. The outside of the outer sleeve is filled with reactor coolant water (light water). At the most upstream position of the vacuum duct, a W disk with a diameter of 46 mm and a thickness of 1 mm is installed as a photon–positron converter. The W disk is surrounded by a cylindrical Cd cap (neutron–photon converter) with a diameter of 62 mm, length of 48 mm, and thickness of 1 mm. The gamma-ray intensity at the positron source is improved through a ^{113}Cd(n,γ)^{114}Cd reaction. By irradiating the W disk with fission gamma-ray photons emitted from the reactor core and neutron capture-induced prompt gamma-ray photons emitted from the Cd cap, positrons are produced inside the W disk and emitted outside. According to a previous simulation study [20], about half of the positrons produced at the KUR positron source are attributed to fission gamma rays emitted from the reactor core. Positrons emitted from the W disk with high energy (~MeV) are incident on W-strip assemblies installed as a positron moderator, and a small fraction is re-emitted into the vacuum with a few eVs of energy. The re-emitted low-energy positrons are extracted by electric bias and guided by a 7-mT magnetic field as a slow positron beam to a sample position. A sample is mounted in a cage that can be applied up to −30 kV, and the incident positron energy to the sample can be varied from 0.1 keV to 30 keV. A slow positron beam with a diameter of about 10 mm and an intensity of 6.2×10^6 e^+/s can be obtained at the sample position during the 5-MW KUR operation. Details regarding the KUR slow positron beamline have been described in other studies [20, 26, 29, 30].

In this study, the amount of positron production was calculated using the particle and heavy ion transport code system (PHITS), a radiation behavior simulation code based on the Monte Carlo technique [31]. Fig. 2 shows a cross-sectional view of the simulation model prepared in this study. The coordinate space of the model is set with the beam axis as the z-axis. The center of the upstream end of the Cd cap is the origin of the coordinate space. The z-direction is defined as the region of -13.3 cm $\leq z \leq$ 60 cm, and both x- and y-directions are defined as the region from −60 cm to 60 cm. In the simulation model, the outer sleeve, inner sleeve, solenoid coils, vacuum duct (made by Al), Cd cap, and W disk are placed in the same way as the actual beamline geometry. The space between the vacuum duct and outer sleeve is filled with air, whereas the outside of the outer sleeve is filled with light water. A planar source with a size of 51×61 cm^2 is placed at $z = -13$ cm (1.2 cm upstream from the tip of the outer sleeve) to simulate the surface of the reactor core. From the planar source, neutrons were emitted with an energy spectrum based on calculations, and gamma-ray photons were emitted with an energy spectrum based on actual measurements [20]. The

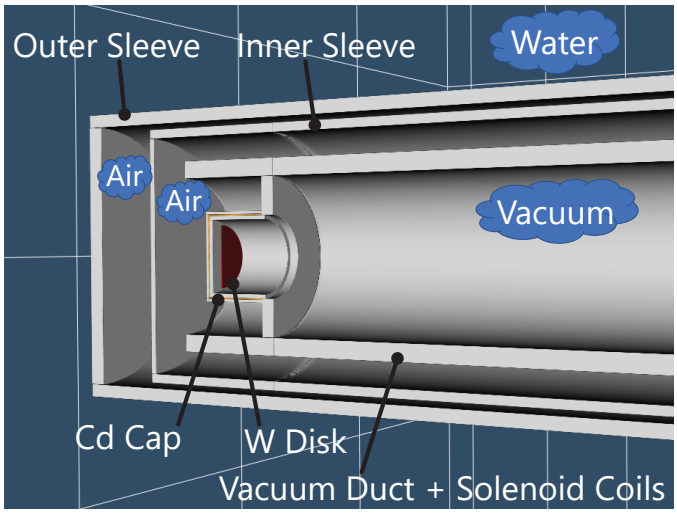

Figure 2: Cross-sectional view of the simulation model. The outer sleeve, inner sleeve, vacuum duct, neutron–photon converter (Cd cap), and W disk with the same geometry as the actual positron source are prepared. The solenoid coils wound on the outside of the vacuum duct are made of Al wires, which is the same material as the vacuum duct and, therefore, are integrated with the vacuum duct in the simulation model. The inside of the outer and inner sleeves is filled with air, whereas the outside of the outer sleeve is filled with light water. A planar source with a size of 51×61 cm^2 is placed at 1.2 cm upstream from the tip of the outer sleeve to simulate the reactor core surface.

fluxes of neutrons and gamma-ray photons at the planar source were used in the calculations as 5.3×10^{12} neutrons/(cm^2·s) and 2.4×10^{12} photons/(cm^2·s), respectively, corresponding to the fluxes at the reactor core surface in the 5-MW KUR operation. Although neutrons and fission gamma-ray photons are emitted from the reactor core simultaneously, the simulation evaluated the amounts of positron production separately for the case where only neutrons are emitted from the planar source and that where only gamma-ray photons are emitted. In each calculation, 4×10^8 neutrons or 2×10^8 gamma-ray photons were emitted from the planar source. Neutron transport calculations were performed until the energy of neutrons became less than 10 μeV. In contrast, transport calculations for photons, electrons, and positrons were excluded when the energy of each particle became less than 10 keV to reduce the calculation time. The PHITS calculations give the number of positrons emitted from the W disk when a single neutron or gamma-ray photon is emitted from the planar source. Since the neutron flux and gamma-ray flux at the reactor core surface (the planar source in the simulation model) are 5.3×10^{12} neutrons/(cm^2·s) and 2.4×10^{12} photons/(cm^2·s), respectively, the planar source with a size of 51×61 cm^2 emits $(51 \times 61) \times (5.3 \times 10^{12})$ neutrons/s and $(51 \times 61) \times (2.4 \times 10^{12})$ photons/s, respectively. By multiplying these values by the number of positrons produced by a single neutron or gamma ray photon, one can obtain the number of positrons emitted from the W disk per unit time. The geometry and calculation method of the simulation is almost the same as in the previous study [20], where more information can be found.

Gamma-ray energy spectra incident on the W disk and the total number of positrons emitted from the W disk into the vacuum when using Cd, Gd, or Sm caps were calculated and compared. In the simulation, all nuclides in the caps were used in their natural abundance with no enrichment. Among the total number of emitted positrons, the amount of positron production induced by fission gamma-ray photons emitted from the reactor core was thought to be almost independent of the cap material; therefore, the number of positrons produced by fission gamma-ray photons was calculated using an Al cap, which is the same material as the vacuum duct.

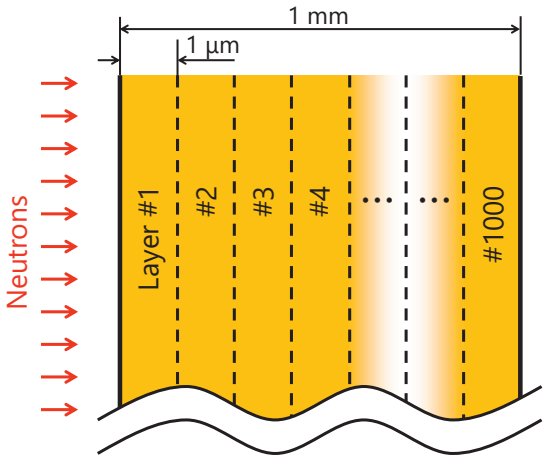

Figure 3: Schematic of a 1-mm-thick cap (disk part at the tip) virtually divided into 1,000 layers.

The burn-up lifetimes of neutron–photon converters made of these three materials when used in the KUR positron source were also evaluated. The lifetime of the disk part at the tip of the cap, which is exposed to the highest neutron flux in the whole cap, was estimated. As shown in Fig. 3, to derive the effective burn-up thickness per unit time for an entire cap, a 1-mm-thick cap was virtually divided into 1000 layers as shown in Fig. 3. The average thermal neutron flux ϕ_0 (cm^{-2}s^{-1}) at the cap surface was assumed by the following equation:

$$\phi_0 = \phi_{5\mathrm{MW}} \times \frac{1.5}{5}, \tag{1}$$

where $\phi_{5\mathrm{MW}}$ (cm^{-2}s^{-1}) is the thermal neutron flux at the reactor core surface in the 5-MW KUR operation (5.3×10^{12} cm^{-2}s^{-1}), and 1.5 means the KUR's average thermal power (1.5 MW). This ϕ_0 is probably an overestimated value as a thermal neutron flux at the surface of the cylindrical-shaped cap, but it was used from the viewpoint of obtaining a short estimate of the burn-up lifetime of the cap. The thermal neutron flux ϕ_i (cm^{-2}s^{-1}) in the i-th layer shown in Fig. 3 was defined by the following equation:

$$\phi_i = \phi_0 \exp\left[-\sigma N (i-1) t\right], \tag{2}$$

where σ (barn) represents the thermal neutron capture cross-section of each nuclide (Table 1), N (cm^{-3}) represents the nuclear density of each nuclide, and t (cm) represents the thickness of each layer (1×10^{-4} cm). The nuclear densities of ^{113}Cd, ^{157}Gd, ^{155}Gd, and ^{149}Sm are 6.5×10^{21} cm^{-3}, 4.6×10^{21} cm^{-3}, 4.4×10^{21} cm^{-3}, and 4.1×10^{21} cm^{-3}, respectively. From the

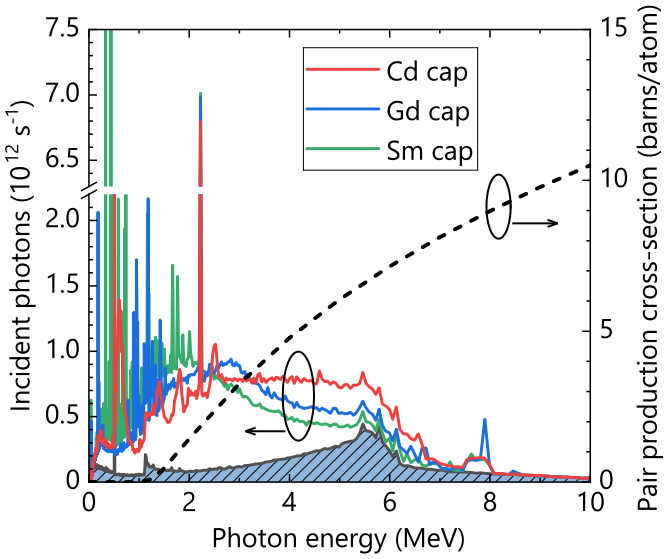

Figure 4: Energy spectra of gamma-ray photons incident on the W disk in the case of using the Cd, Gd, or Sm cap when both neutrons and gamma-ray photons are emitted from the planar source (solid lines). The hatched area corresponds to the energy spectrum of gamma-ray photons incident on the W disk when only gamma-ray photons are emitted from the planar source, which is a common spectrum, regardless of the cap material. The pair production cross-section for gamma-ray photons in W, drawn on the basis of the NIST database [32], is indicated by the dashed line.

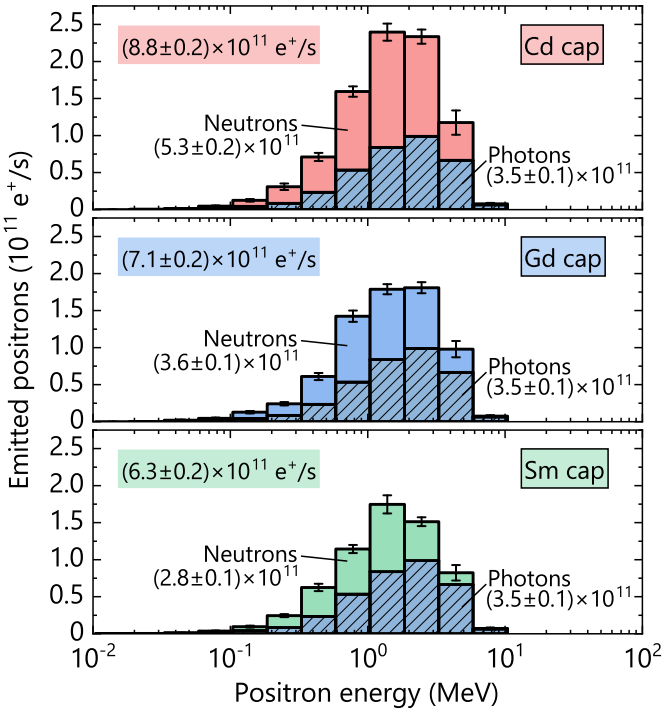

Figure 5: Number of positrons emitted from the W disk into a vacuum per unit time when both neutrons and gamma-ray photons were emitted from the planar source. The upper, middle, and lower panels show the cases using the Cd, Gd, and Sm caps, respectively. "Neutrons", "Photons", and the values under each label represent the numbers of positrons attributed to neutron capture-induced prompt gamma-ray photons and fission gamma-ray photons, respectively. The total number of emitted positrons in the cases using each cap is also indicated in the upper left corner of each panel.

above, the burn-up per unit time in the i-th layer in the initial burning stage can be obtained by the following equation:

$$\frac{\phi_i \sigma N t}{N t} = \phi_i \sigma. \tag{3}$$

Therefore, the effective burn-up thickness of each layer per unit time is given by $\phi_i \sigma t$, and the effective burn-up thickness of the entire cap per unit time t_{eff} is given by

$$t_{\mathrm{eff}} = \sum_{i=1}^{1000} \phi_i \sigma t. \tag{4}$$

Using the effective burn-up rates, the required time for the effective thickness of each cap to reach the minimum thickness necessary to maintain its initial performance as a neutron–photon converter was evaluated. The minimum thickness required to maintain the initial performance was defined as the thickness required to capture 99% of thermal neutrons.

3. Results

Fig. 4 shows the calculated energy spectra of the gamma-ray photons incident on the W disk when both neutrons and gamma-ray photons are emitted from the planar source. The hatched area at the bottom is the energy spectra of gamma-ray photons incident on the W disk when only gamma-ray photons are emitted from the planar source. The hatched baseline is common to the three types of caps. The amounts of photons added to the baseline correspond to the spectra of gamma-ray photons incident on the W disk when only neutrons are emitted from the planar source. The pair production cross-section in W drawn on the basis of the NIST database [32] is indicated by the dashed line in Fig. 4. In the high-energy region of 3–7 MeV, where the pair production cross-section is large, the gamma-ray intensity is different depending on the cap material. In the high-energy region, the number of gamma-ray photons per unit time incident on the W disk decreases in the order of Cd, Gd, and Sm caps. However, regardless of the cap material, a sharp peak is observed at 2.2 MeV. The integral values of the product of the intensity of gamma-ray photons and the pair production cross-section for respective energies are summarized in Table 2.

Fig. 5 shows the calculated results of the number of positrons emitted from the W disk per unit time for each cap. The hatched area at the bottom of each panel is the number of positrons emitted from the W disk when only gamma-ray photons are emitted from the planar source. The area above the hatched area corresponds to the number of positrons emitted from the W disk only when neutrons are emitted from the planar source. The number of positrons emitted from the W disk per unit time when only neutrons are emitted from the planar source is estimated to be $(5.3 \pm 0.2) \times 10^{11}$ e$^+$/s, $(3.6 \pm 0.1) \times 10^{11}$ e$^+$/s, and $(2.8 \pm 0.1) \times 10^{11}$ e$^+$/s with the Cd, Gd, and Sm caps, respectively. The number of positrons emitted from the W disk per unit time decreases in the order of Cd, Gd, and Sm caps. In the upper left of each panel in Fig. 5, the total number of positrons

Table 2: Integral values of the product of the intensity of gamma-ray photons and the pair production cross-section for respective energies. The terms "n+γ total" and "n only" refer to the case where both fission gamma-ray photons and neutron-induced gamma-ray photons are incident on the W disk, and the case where only neutron-induced gamma-ray photons are incident on the W disk, respectively. The ratio of each integral value to the value with the Cd cap is also shown on the right side of the table.

	Integral value of the product			Ratio to using Cd cap		
	Cd cap	Gd cap	Sm cap	Cd cap	Gd cap	Sm cap
n+γ total	1.92×10^{13}	1.63×10^{13}	1.38×10^{13}	1	0.85	0.72
n only	1.22×10^{13}	9.25×10^{12}	6.82×10^{12}	1	0.76	0.56

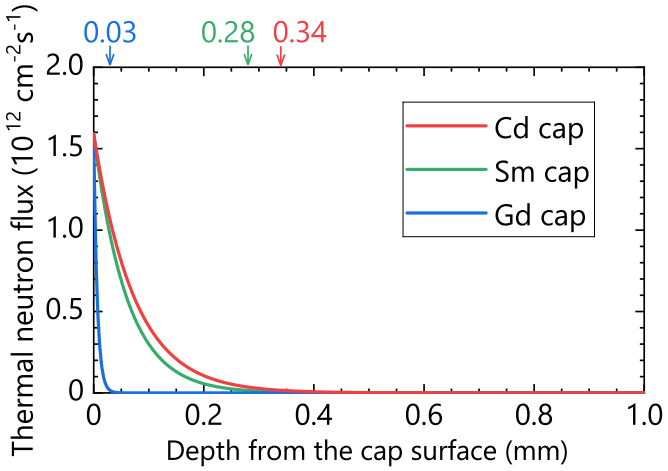

Figure 6: Thermal neutron flux distributions inside the cap. On the upper axis, the required thickness for the Cd, Sm, and Gd caps to capture 99% of the thermal neutrons is indicated in red, green, and blue, respectively.

emitted from the W disk per unit time is indicated.

Fig. 6 shows the thermal neutron flux distributions inside each cap calculated by Equation (2), *i.e.*, the attenuation of thermal neutrons inside the cap. The value of thermal neutron flux at the cap surface (1.59×10^{12} cm^{-2}s^{-1}) was adopted on the basis of the value of thermal neutron flux at the reactor core surface at the KUR's average thermal power (1.5 MW). Since the cap is located 13 cm downstream from the surface of the core, the adopted thermal neutron flux is a slightly more severe condition for the burn-up lifetime of the cap. Among the three caps, the attenuation of thermal neutrons is the most gradual in the Cd cap, which has the smallest thermal neutron capture cross-section. In contrast, thermal neutrons attenuate most steeply in the Gd cap, which has the largest thermal neutron capture cross-section. The required thicknesses for the Cd, Gd, and Sm caps to absorb 99% of thermal neutrons are 0.34, 0.03, and 0.28 mm, respectively. The effective burn-up thicknesses per unit time $\sum_{i=1}^{1000} \phi_i \sigma t$ of each cap burned with the KUR's average thermal power of 1.5 MW were calculated and are summarized in Table 3. For the three caps, the effective thickness decreased by ~10 nm per hour.

Table 3: Effective burn-up thicknesses per unit time for each cap material burned in the KUR positron source with an average thermal neutron flux of 1.59×10^{12} neutrons/(cm^{2}s).

Cap material	Burn-up rate (mm/h)
Cd	8.76×10^{-6}
Sm	1.39×10^{-5}
Gd	1.24×10^{-5}

4. Discussion

As shown in Fig. 5, the total number of positrons emitted from the W disk when using the Cd cap is $(8.8\pm0.2)\times10^{11}$ e$^+$/s. This value is comparable to the result of the previous study [20]. When the Cd cap is replaced with a Gd cap, the total number of positrons decreases to $(7.1 \pm 0.2) \times 10^{11}$ e$^+$/s (81±3% compared to the Cd cap), and when it is replaced with a Sm cap, the total number of positrons decreases to $(6.3 \pm 0.2) \times 10^{11}$ e$^+$/s (72±3% compared to the Cd cap). This decreasing tendency is consistent with that estimated from the product of the gamma-ray intensity incident on the W disk and the pair production cross-section ("n+γ total" in Table 2).

Among the number of positrons emitted from the W disk when using the Cd cap, the number of positrons produced from the neutron-induced gamma-ray photons is $(5.3\pm0.2)\times10^{11}$ e$^+$/s as shown in Fig. 5. When the Cd cap is replaced by the Gd or Sm cap, the number of positrons induced by neutrons become $(3.6 \pm 0.1) \times 10^{11}$ e$^+$/s and $(2.8 \pm 0.1) \times 10^{11}$ e$^+$/s, which are decreased to (69 ± 4)% and (54 ± 3)%, respectively, compared to when the Cd cap is used. This decreasing tendency is also consistent with that estimated from the product of the gamma-ray photon intensity and the pair production cross-section ("n only" in Table 2). This difference is considered to reflect the difference in the energy spectrum of gamma-ray photons incident on the W disk, as shown in Fig. 4. The intensity of high-energy (3–7 MeV) gamma-ray photons incident on the W disk is the highest when using the Cd cap. As high-energy gamma-ray photons have large pair production cross-sections, the number of emitted positrons is the highest when using the Cd cap. The calculation results show that the total number of positrons obtained by using Gd or Sm caps instead of a Cd cap will be significantly reduced, especially in high neutron flux reactors. However, if effective cooling of the neutron–photon converter

is inevitably difficult due to the structure of the positron source, a Gd cap may be useful despite the amount of positron production being reduced. Meanwhile, the sharp peak observed at 2.2 MeV in Fig. 4 can be attributed to the ^{1}H(n,γ)^{2}H reaction in the coolant water. The previous study [20] has visualized that the gamma-ray intensity is improved in the coolant water even when only neutrons are emitted from a planar source.

Then, the lifetimes of each cap as a neutron–photon converter when they are burned at the KUR positron source are considered. The required thicknesses for the Cd, Sm, and Gd caps to capture 99% of the thermal neutrons are 0.34, 0.28, and 0.03 mm, respectively, as shown in Fig. 6. Therefore, the burn-up lifetimes of each cap are defined as the durations until the effective burn-up thicknesses t_{eff} of the Cd, Sm, and Gd caps with a physical thickness of 1 mm become $(1 - 0.34)$ mm, $(1 - 0.28)$ mm, and $(1 - 0.03)$ mm, respectively. The effective burn-up rates of each cap burned at the KUR's average thermal power are summarized in Table 3. Based on these values, the times required for the effective burn-up thickness of the Cd, Sm, and Gd caps to reach 0.66, 0.72, and 0.97 mm are calculated to be 75342, 51799, and 78226 h, respectively. Assuming the annual operation time of the KUR is 1000 h, the burn-up lifetimes of the Cd, Sm, and Gd caps are 75, 52, and 78 years, respectively, *i.e.*, the three caps have sufficient burn-up lifetimes of more than 50 years. In addition, Cd and Gd caps with a thickness of 1 mm have almost the same burn-up lifetime. However, these burn-up lifetimes would be significantly shorter if the caps are used in a higher thermal neutron flux environment. A 3-mm-thick Cd cap enriched with 80% ^{113}Cd is adopted in the FRM-II positron source to extend the replacement lifetime of the cap [18, 33].

5. Conclusion

In this study, positron production in the KUR slow positron beamline using Gd or Sm caps instead of a Cd cap was simulated using the PHITS code. Based on the simulation results, the amounts of positron production induced by neutrons when using Gd or Sm caps were estimated to be (69 ± 4)% and (54 ± 3)% of what would be obtained with a Cd cap. Therefore, in terms of maximizing the amount of positron production, a Cd cap is the best choice as a neutron–photon converter. However, as Gd has a significantly higher melting point than Cd, if effective cooling is difficult due to the structure of the positron source, a Gd cap may be a good alternative despite the amount of positron production being reduced. All non-enriched Cd, Gd, and Sm caps with a 1-mm thickness have sufficient burn-up lifetimes of more than 50 years as long as they are burned in the KUR positron source. If they are to be used under higher thermal neutron fluxes, an increase in cap thickness and/or enrichment of neutron capture nuclides will be required to extend the replacement lifetimes of these caps.

References

[1] P. J. Schultz, K. G. Lynn, Interaction of positron beams with surfaces, thin films, and interfaces, Rev. Mod. Phys. 60 (1988) 701. doi:10.1103/RevModPhys.60.701.

[2] F. Tuomisto, I. Makkonen, Defect identification in semiconductors with positron annihilation: Experiment and theory, Rev. Mod. Phys. 85 (2013) 1583. doi:10.1103/RevModPhys.85.1583.

[3] J. Čížek, Characterization of lattice defects in metallic materials by positron annihilation spectroscopy: A review, J. Mater. Sci. Technol. 34 (2018) 577. doi:10.1016/j.jmst.2017.11.050.

[4] F. A. Selim, Positron annihilation spectroscopy of defects in nuclear and irradiated materials—a review, Mater. Charact. 174 (2021) 110952. doi:10.1016/j.matchar.2021.110952.

[5] C. Piochacz, W. Egger, C. Hugenschmidt, G. Kögel, K. Schreckenbach, P. Sperr, G. Dollinger, Implementation of the munich scanning positron microscope at the positron source NEPOMUC, Phys. Status Solidi C 4 (2007) 4028. doi:10.1002/pssc.200675824.

[6] M. Maekawa, A. Kawasuso, Construction of a positron microbeam in JAEA, Appl. Surf. Sci. 255 (2008) 39. doi:10.1016/j.apsusc.2008.05.180.

[7] N. Oshima, R. Suzuki, T. Ohdaira, A. Kinomura, T. Narumi, A. Uedono, M. Fujinami, Development of Positron Microbeam in AIST, Mater. Sci. Forum 607 (2008) 238. doi:10.4028/www.scientific.net/MSF.607.238.

[8] N. Oshima, R. Suzuki, T. Ohdaira, A. Kinomura, T. Narumi, A. Uedono, M. Fujinami, A positron annihilation lifetime measurement system with an intense positron microbeam, Radiat. Phys. Chem. 78 (2009) 1096. doi:10.1016/j.radphyschem.2009.06.035.

[9] T. Gigl, L. Beddrich, M. Dickmann, B. Rienäcker, M. Thalmayr, S. Vohburger, C. Hugenschmidt, Defect imaging and detection of precipitates using a new scanning positron microbeam, New J. Phys. 19 (2017) 123007. doi:10.1088/1367-2630/aa915b.

[10] Y. Fukaya, M. Maekawa, A. Kawasuso, I. Mochizuki, K. Wada, T. Shidara, A. Ichimiya, T. Hyodo, Total reflection high-energy positron diffraction: An ideal diffraction technique for surface structure analysis, Appl. Phys. Express 7 (2014) 056601. doi:10.7567/APEX.7.056601.

[11] Y. Fukaya, A. Kawasuso, A. Ichimiya, T. Hyodo, Total-reflection high-energy positron diffraction (TRHEPD) for structure determination of the topmost and immediate sub-surface atomic layers, J. Phys. D: Appl. Phys. 52 (2019) 013002. doi:10.1088/1361-6463/aadf14.

[12] M. Dodenhöft, S. Vohburger, C. Hugenschmidt, Development of a new reflection high-energy positron diffractometer at NEPOMUCf, AIP Conf. Proc. 2182 (2019) 040003. doi:10.1063/1.5135835.

[13] B. Krusche, K. Schreckenbach, Intense positron sources by pair creation with neutron capture γ-rays, Nucl. Instrum. Methods Phys. Res., Sect. A 295 (1990) 155. doi:10.1016/0168-9002(90)90435-9.

[14] G. Triftshäuser, G. Kögel, W. Triftshäuser, M. Springer, B. Strasser, K. Schreckenbach, A high intense reactor based positron source, Appl. Surf. Sci. 116 (1997) 45. doi:10.1016/S0169-4332(96)00972-5.

[15] C. Hugenschmidt, G. Kögel, R. Repper, K. Schreckenbach, P. Sperr, B. Straßer, W. Triftshäuser, Monoenergetic positron beam at the reactor based positron source at FRM-II, Nucl. Instrum. Methods Phys. Res., Sect. B 192 (2002) 97. doi:10.1016/S0168-583X(02)00788-7.

[16] C. Hugenschmidt, G. Kögel, R. Repper, K. Schreckenbach, P. Sperr, W. Triftshäuser, First platinum moderated positron beam based on neutron capture, Nucl. Instrum. Methods Phys. Res., Sect. B 198 (2002) 220. doi:10.1016/S0168-583X(02)01527-6.

[17] A. G. Hathaway, M. Skalsey, W. E. Frieze, R. S. Vallery, D. W. Gidley, A. I. Hawari, J. Xu, Implementation of a prototype slow positron beam at the NC State University PULSTAR reactor, Nucl. Instrum. Methods Phys. Res., Sect. A 579 (2007) 538. doi:10.1016/j.nima.2007.03.036.

[18] C. Hugenschmidt, C. Piochacz, M. Reiner, K. Schreckenbach, The NEPOMUC *upgrade* and advanced positron beam experiments, New J. Phys. 14 (2012) 055027. doi:10.1088/1367-2630/14/5/055027.

[19] A. Zeman, K. Tuček, L. Debarberis, A. Hogenbirk, High intensity positron source at HFR: Basic concept, scoring and design optimisation, Nucl. Instrum. Methods Phys. Res., Sect. B 271 (2012) 19. doi:10.1016/j.nimb.2011.10.003.

[20] A. Yabuuchi, T. Yoshiie, A. Kinomura, Contribution of cadmium to the total amount of positron creation in a reactor-based slow positron beamline, Nucl. Instrum. Methods Phys. Res., Sect. B 463 (2020) 40. doi:10.1016/j.nimb.2019.11.028.

[21] D. Pal, S. Mukherjee, P. Maheshwari, S. K. Sharma, D. Dutta, K. Sudarshan, R. G. Thomas, P. K. Pujari, Design parameters of proposed intense positron facility at Mumbai research reactor, AIP Conf. Proc. 2265 (2020)

030208. doi:10.1063/5.0017864.

[22] A. van Veen, H. Schut, F. Labohm, J. de Roode, Positron extraction and transport in a nuclear-reactor-based positron beam, Nucl. Instrum. Methods Phys. Res., Sect. A 427 (1999) 266. doi:10.1016/S0168-9002(98)01517-4.

[23] G. Wang, R. Li, D. Qian, X. Yang, Physical models and primary design of reactor based slow positron source at CMRR, Nucl. Instrum. Methods Phys. Res., Sect. B 427 (2018) 38. doi:10.1016/j.nimb.2018.04.022.

[24] McMaster Intense Positron Beam Facility, https://nuclear.mcmaster.ca/facility/mipbf/.

[25] R. Alsulami, M. A. an S. Jaradat, S. Usman, J. Graham, Optimizing the moderator geometry and thickness for a reactor-based slow positron source, Nucl. Instrum. Methods Phys. Res., Sect. B 497 (2021) 39. doi:10.1016/j.nimb.2021.04.005.

[26] A. Yabuuchi, R. Naka, K. Sato, Q. Xu, A. Kinomura, Slow-positron beamline temperature rise reduction at Kyoto University Research Reactor, Nucl. Instrum. Methods Phys. Res., Sect. B 461 (2019) 137. doi:10.1016/j.nimb.2019.09.036.

[27] A. G. Hathaway, Design and Testing of a Prototype Slow Positron Beam at the NC State University PULSTAR Reactor, Master's thesis, North Carolina State University (2005).

[28] Japan Radioisotope Association (Ed.), Radioisotope Pocket Data Book, 11th Edition, Maruzen, 2011.

[29] K. Sato, Q. Xu, T. Yoshiie, T. Sano, H. Kawabe, Y. Nagai, K. Nagumo, K. Inoue, T. Toyama, N. Oshima, A. Kinomura, Y. Shirai, Development of a mono-energetic positron beam line at the Kyoto University Research Reactor, Nucl. Instrum. Methods Phys. Res., Sect. B 342 (2015) 104. doi:10.1016/j.nimb.2014.09.022.

[30] Q. Xu, K. Sato, T. Yoshiie, T. Sano, H. Kawabe, Y. Nagai, K. Nagumo, K. Inoue, T. Toyama, N. Oshima, A. Kinomura, Y. Shirai, Positron beam facility at Kyoto University Research Reactor, J. Phys.: Conf. Ser. 505 (2014) 012030. doi:10.1088/1742-6596/505/1/012030.

[31] T. Sato, Y. Iwamoto, S. Hashimoto, T. Ogawa, T. Furuta, S. Abe, T. Kai, P. E. Tsai, N. Matsuda, H. Iwase, N. Shigyo, L. Sihver, K. Niita, Features of Particle and Heavy Ion Transport code System (PHITS) version 3.02, J. Nucl. Sci. Technol. 55 (2018) 684. doi:10.1080/00223131.2017.1419890.

[32] XCOM: Photon Cross Sections Database, https://www.nist.gov/pml/xcom-photon-cross-sections-database/.

[33] C. Hugenschmidt, The status of the positron beam facility at NEPOMUC, J. Phys.: Conf. Ser. 262 (2011) 012002. doi:10.1088/1742-6596/262/1/012002.